



Cite this: DOI: 10.1039/c8dt02683a

# Simulating the effect of a triple bond to achieve the shortest main group metal–metal distance in diberyllium complexes: a computational study†

Xue-Feng Zhao,<sup>a</sup> Caixia Yuan,<sup>a</sup> Si-Dian Li,<sup>b</sup> Yan-Bo Wu<sup>\*a</sup> and Xiaotai Wang<sup>ib</sup><sup>\*b</sup>

The subject of metal–metal bonding interactions in molecular systems continues to attract research interest. Chromium heretofore has been the only element known to afford metal–metal distances shorter than 1.700 Å in the form of Cr–Cr multiple bonds. In this computational study, the effect of a triple bond on reducing interatomic distances is simulated through forming three non-classical bonding orbitals between two beryllium atoms, thereby realizing the remarkably short Be–Be distances (1.692–1.735 Å) in kinetically stable global minimum species  $[L \rightarrow \text{Be}_2\text{H}_3 \leftarrow L]^+$  ( $L = \text{NH}_3, \text{PH}_3,$  and noble gases Ne–Xe). Such diberyllium complexes make promising candidates for experimental realization. In particular, the Be–Be distance of 1.692 Å in  $[\text{Ne} \rightarrow \text{Be}_2\text{H}_3 \leftarrow \text{Ne}]^+$  represents the first example of global minimum having a main group metal–metal distance under 1.700 Å.  $[\text{TEA} \rightarrow \text{Be}_2\text{H}_3 \leftarrow \text{TEA}]^+$ , which contains the bulky triethylamine (TEA) ligands, is designed as a more promising target for synthesis and isolation in condensed states.

Received 2nd July 2018,  
Accepted 20th August 2018

DOI: 10.1039/c8dt02683a

rsc.li/dalton

## Introduction

Studies on the interaction between metal atoms in discrete molecular systems continue to expand our understanding of the nature of chemical bonding.<sup>1</sup> An intriguing question is how short a metal–metal distance could become. Such an interatomic distance generally decreases with increasing numbers of bonding orbitals between the atoms. It is well known that transition metals with an appropriate number of valence electrons in d orbitals can achieve short metal–metal distances by forming high-order multiple bonds *via* the strong interaction between the d orbitals.<sup>2</sup> Research on this subject dates back to the seminal discovery in 1964 of the quadruple metal–metal bond (2.24 Å) in  $[\text{Re}_2\text{Cl}_8]^{2-}$  by Cotton and co-workers.<sup>3</sup> The most significant recent developments have been the realization of ultrashort metal–metal bond distances defined as  $d_{\text{M-M}} < 1.900 \text{ \AA}$ , and examples include the crystallo-

graphically determined quintuple Cr–Cr bonds ranging from 1.835 to 1.706 Å,<sup>4</sup> as well as a spectroscopically characterized sextuple Cr–Cr bond in dichromium ( $\text{Cr}_2$ ) at 1.679 Å.<sup>5</sup> In addition, a computational study has predicted that the quintuple Cr–Cr bond in  $\text{FCrCrF}$  would have a distance of 1.650 Å.<sup>6</sup> This has been so far the shortest of any experimentally or theoretically known metal–metal distances.

In comparison, it is more challenging to achieve ultrashort metal–metal distances between main group elements because of the nature of their valence shell electronic structures. The s-block metals do not have enough valence electrons, whereas the p-block metals suffer from the so-called inert pair effect that prevents the outmost s lone pairs from participating in bonding.<sup>7</sup> Nonetheless, the alkaline earth metal beryllium, on account of its unique properties, stands out as a viable source of ultrashort metal–metal distances. Beryllium has the smallest atomic radius of any metals. Furthermore, the high electron deficiency of beryllium allows the furnishing of auxiliary electron-donating atoms between two beryllium centers to maximize the number of bonding orbitals. Thus, it is possible to realize ultrashort Be–Be distances rivaling those of quintuple bonds between transition metal (chromium) atoms.

Recent computational studies have provided support for the above proposition. For example, the Ding and Frenking group reported the Be–Be distances of 1.910 and 1.901 Å in the molecular discuses  $D_{7h} \text{Be}_2\text{B}_7^-$  and  $D_{8h} \text{Be}_2\text{B}_8$ , which approach the

<sup>a</sup>Key Laboratory of Materials for Energy Conversion and Storage of Shanxi Province, Institute of Molecular Science, Shanxi University, Taiyuan, 030006, People's Republic of China. E-mail: wyb@sxu.edu.cn

<sup>b</sup>Department of Chemistry, University of Colorado Denver, Campus Box 194, P.O. Box 173364, Denver, Colorado 80217-3364, USA.

E-mail: Xiaotai.wang@ucdenver.edu

† Electronic supplementary information (ESI) available: The AdNDP results of 4–10, the pictures of optimized structures and relative energies of lowest isomers of 3–10, and the Cartesian coordinates of structures shown in the figures in the text. See DOI: 10.1039/c8dt02683a

upper limit of ultrashort metal–metal distances.<sup>8</sup> We computed novel species containing ultrashort metal–metal distances (1.728–1.866 Å) between two Be atoms in different molecular environments, including a rhombic Be<sub>2</sub>X<sub>2</sub> (X = C, N) core and a Be–Be axis supported by a peripheral (BeH)<sub>n</sub> (n = 5 or 6) star-like frame or two N-heterocyclic carbene (NHC) ligands.<sup>9</sup> More recently, the Zhou and Frenking group designed beryllium noble gas (Ng) complexes of the type Ng → Be<sub>2</sub>O<sub>2</sub> ← Ng with ultrashort Be–Be distances (1.736–1.763 Å).<sup>10</sup>

Thus far the shortest Be–Be distance (1.728 Å) has been that in Be<sub>2</sub>(NLi)<sub>2</sub>, a computationally designed global minimum reported by our group in 2016.<sup>9</sup> Would it be possible to design diberyllium complexes with Be–Be distances under 1.700 Å, which would rival those of the shortest multiple bonds between two transition metal (Cr) atoms? The answer is positive and presented in the current computational study, which leverages (a) the maximum number of bonding orbitals between two Be atoms and (b) the minimum steric effect of terminal ligands.

### Computational methods

Two mixed basis sets were used in this work: BS1 denotes aug-cc-pVQZ-PP for Xe and aug-cc-pVQZ for other elements, and BS2 denotes SDD for Xe and 6-31G(d) for other elements. The small structures of **1–10** were computed at both B3LYP/BS1 and MP2/BS1 levels, which gave similar geometries and vibrational frequencies; the large structure **11** was computed only at the B3LYP/BS1 level. The geometries of **1–10** were further refined at the CCSD(T)/BS1 level. Adaptive natural density partitioning (AdNDP)<sup>11</sup> and natural bond orbital (NBO)<sup>12</sup> analyses were performed at the B3LYP/BS2 and B3LYP/BS1 levels, respectively. Vertical detachment energies (VDEs) and vertical electron affinities (VEAs) were calculated using outer-valence Green's functions (OVGF)<sup>13</sup> for **3–10** at the OVGF/BS1 level. The benchmark calculation for **3** at the OVGF/aug-cc-pVDZ level gave essentially identical VDE and VEA to those obtained at the OVGF/BS1 level, so the VDE and VEA of the large molecule **11** were calculated at the OVGF/aug-cc-pVDZ level. The potential energy surface of each of **3–10** was explored using a stochastic search algorithm,<sup>14</sup> with the initial random structures optimized at the B3LYP/BS2 level and the 10 lowest-energy isomers re-optimized and their frequencies calculated at the B3LYP/BS1 level. The five lowest-energy isomers at the B3LYP/BS1 level were identified and their energies were further improved at the CCSD(T)/BS1 level. The relative free energies of these five isomers were compared using CCSD(T)/BS1 electronic energies plus B3LYP/BS1 Gibbs free energy corrections. The 100-picosecond Born-Oppenheimer molecular dynamic (BOMD)<sup>15</sup> simulations were carried out for **3**, **4**, and **6–9** at the B3LYP/BS2 level and 298 K. The stochastic search was realized using the GXYZ program,<sup>16</sup> the AdNDP analyses were performed using the AdNDP program,<sup>17</sup> the CCSD(T) calculations were carried out using the MolPro 2012.1 package,<sup>18</sup> and all other calculations were performed using the Gaussian 09 package.<sup>19</sup>

## Results and discussion

### [L → Be<sub>2</sub>H<sub>3</sub> ← L]<sup>+</sup> (L = NH<sub>3</sub>, PH<sub>3</sub>) with three Be–H–Be bonds

We have recently reported [NH<sub>3</sub> → Be<sub>2</sub>H<sub>2</sub>CH<sub>2</sub> ← NH<sub>3</sub>] (**1**) and [PH<sub>3</sub> → Be<sub>2</sub>H<sub>2</sub>CH<sub>2</sub> ← PH<sub>3</sub>] (**2**), two computationally designed and characterized diberyllium complexes with respective ultrashort Be–Be distances of 1.791 and 1.766 Å (Fig. 1).<sup>20</sup> In **1** and **2**, each Be atom is supported by a terminal ammonia/phosphine ligand, and the two Be centers are bridged by two H atoms and a –CH<sub>2</sub>– group. The ultrashort Be–Be distances in **1** and **2** are achieved by the combined effects of forming two Be–H–Be 3c–2e bonds and having favorable coulombic attractions between the negatively charged carbon atom of the –CH<sub>2</sub>– group and the positively charged beryllium atoms. In the present study, we envisioned that using a H atom to replace the –CH<sub>2</sub>– group in **1** and **2** could result in cationic complexes [L → Be<sub>2</sub>H<sub>3</sub> ← L]<sup>+</sup> with three Be–H–Be 3c–2e bonds to further decrease the Be–Be distance. This idea has been realized with the computation of D<sub>3h</sub> [NH<sub>3</sub> → Be<sub>2</sub>H<sub>3</sub> ← NH<sub>3</sub>]<sup>+</sup> and [PH<sub>3</sub> → Be<sub>2</sub>H<sub>3</sub> ← PH<sub>3</sub>]<sup>+</sup> (**3** and **4** in Fig. 1) as energy minima at both B3LYP/BS1 and MP2/BS1 levels of theory. The geometries of **3** and **4** have been refined at the higher CCSD(T)/BS1 level

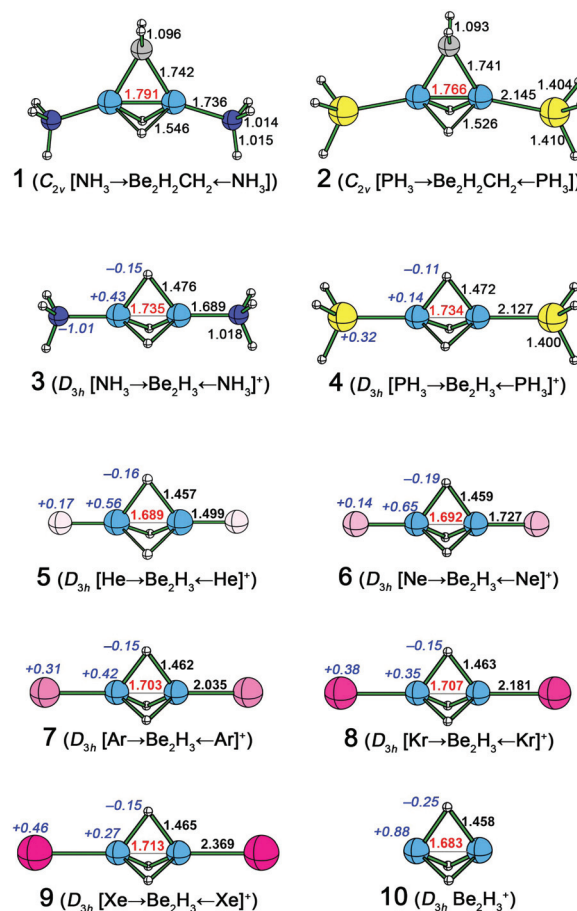


Fig. 1 CCSD(T)/BS1-optimized structures of **1–10**, with Be–Be distances, other interatomic distances, and NBO charges given in red, black, and italic blue fonts, respectively.

to give the Be–Be distances of 1.735 and 1.734 Å, respectively, which are close to the shortest Be–Be distance of 1.728 Å in  $\text{Be}_2(\text{NLi})_2$ .<sup>9</sup>

To gain insight into the ultrashort Be–Be distances in **3** and **4**, we have performed a detailed bonding analysis using the AdNDP method. Developed as an extension of NBO analysis, AdNDP describes the electronic structure of a molecular system in terms of  $n$ -center two-electron ( $nc$ -2e) bonds or orbitals ( $n$  ranges from one to the total number of atoms), and as such, it reveals not only classical Lewis bonding elements, including lone pairs and 2c-2e bonds, but also nonclassical delocalized  $nc$ -2e bonds. We employed two equivalent partitioning schemes for the AdNDP analysis to gain alternative representations of the bonding between the atoms in **3** and **4** (Fig. 2 in the main text and Fig. S1 in the ESI†). With one scheme, we generated AdNDP orbitals with the smallest possible  $n$  values, as shown in Fig. 2, which translate into three Be–H–Be 3c-2e  $\sigma$  bonds (A–C) and two N  $\rightarrow$  Be dative 2c-2e  $\sigma$  bonds (D and E) for **3**, all of them having an occupation

number (ON) of 1.99|e|. The Be–H–Be 3c-2e bonds are similar to the B–H–B 3c-2e bonds known in diborane.<sup>21</sup> Use of the other partitioning scheme led to retention of the two N  $\rightarrow$  Be dative 2c-2e  $\sigma$  bonds (D' and E'), and transformation of the three Be–H–Be 3c-2e  $\sigma$  bonds into three 5c-2e bonds (F, G, and H). H is a  $\sigma$ -shaped orbital without any nodes between the beryllium atoms, whereas F and G are degenerate orthogonal  $\pi$ -shaped orbitals, each having a nodal surface passing the Be–Be axis. The orbital set of F, G, and H may be viewed as a nonclassical counterpart of a classical triple bond (e.g.,  $\text{C}\equiv\text{C}$ ). This provides another explanation for the further shortening of the Be–Be distance in **3**.

The above bonding analysis also reveals an isolobal relationship between **3** and 2-butyne, as shown in Fig. 2. Both **3** and 2-butyne have 22 valence electrons, 12 of them forming six N–H/C–H orbitals, another four forming two N–Be/C–C orbitals (orbitals D' and E' vs. L and M), and the remaining six forming the three bonding orbitals between two beryllium/carbon atoms (orbitals F, G, and H vs. orbitals I, J, and K). Clearly, the corresponding orbitals in **3** and 2-butyne have similar shapes and symmetry properties.

We have also performed standard NBO analyses to further characterize **3** and **4**. The resulting Wiberg bond indices (WBI) and natural charges, which are descriptors of covalent and ionic bonding, are given in Table 1 and Fig. 1, respectively. The total WBI values per beryllium atom are 2.51 and 2.85 in **3** and **4**, respectively, which are greater than two, the number of beryllium valence electrons. The exceeding values of 0.51 and 0.85 are close to the  $\text{WBI}_{\text{Be-N}}$  and  $\text{WBI}_{\text{Be-P}}$  values of 0.50 and 0.78, respectively, which support the dative nature of the N  $\rightarrow$  Be and P  $\rightarrow$  Be bonds. In addition, the  $\text{WBI}_{\text{Be-N}}$  of 0.50 for **3** suggests relatively weak Be–N covalent interaction due to the large difference in the electronegativities of Be and N. This weakness in covalency, however, is compensated for by relatively strong Be–N electrostatic attraction, as reflected by the natural charges  $Q_{\text{N}} = -1.01|e|$  and  $Q_{\text{Be}} = +0.43|e|$  (Fig. 1). In comparison, the  $\text{WBI}_{\text{Be-P}}$  value is 0.78 in **4**, suggesting a largely covalent Be–P interaction. In both **3** and **4**, the  $\text{WBI}_{\text{Be-H}}$  is 0.48, and given that there are a total of three bridging H

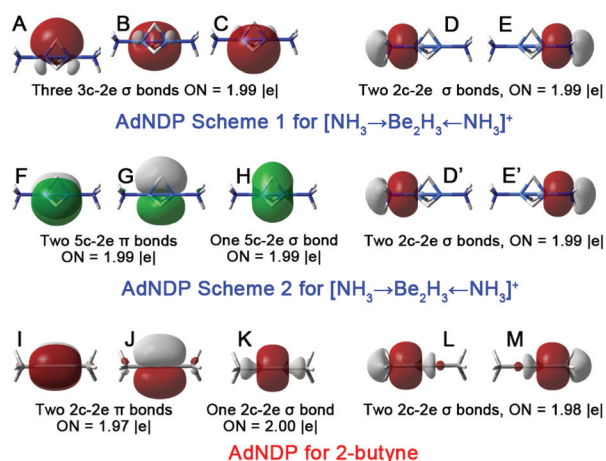


Fig. 2 AdNDP-generated orbitals for bonding to beryllium in **3** (top and middle) and for bonding to sp-carbon in 2-butyne (bottom). Analogous AdNDP orbitals for **4** are shown in Fig. S1.†

Table 1 The lowest vibrational frequencies ( $\nu_{\text{min}}$  in  $\text{cm}^{-1}$ ), the HOMO–LUMO gaps (gap in eV), the VDEs and VEAs (in eV), and the Wiberg bond indices (WBIs) for selected atoms and atom–atom interactions

	$\nu_{\text{min}}$	Gap	VDE	VEA	WBI					
					Be	H	E	Be–Be	Be–H	Be–E
<b>3</b>	74	7.65	15.20 15.14 <sup>a</sup>	–2.86 –2.86 <sup>a</sup>	2.51	0.98	2.92	0.55	0.48	0.50
<b>4</b>	51	7.50	15.15	–2.56	2.85	0.99	3.75	0.59	0.48	0.78
<b>5</b>	170	8.51	18.10	–3.68	2.31	0.98	0.32	0.54	0.48	0.31
<b>6</b>	102	7.79	17.81	–4.30	2.19	0.97	0.26	0.50	0.48	0.25
<b>7</b>	92	8.14	16.90	–3.32	2.52	0.98	0.56	0.54	0.48	0.53
<b>8</b>	81	7.93	16.52	–2.81	2.62	0.98	0.65	0.54	0.48	0.62
<b>9</b>	74	7.75	15.98	–2.67	2.72	0.98	0.76	0.54	0.48	0.72
<b>10</b>	1044	6.23	18.57	–6.68	1.83	0.94		0.44	0.47	
<b>11</b>	16	8.38	13.91 <sup>a</sup>	–1.81 <sup>a</sup>						

<sup>a</sup> These values are calculated at the OVGF/aug-cc-pVDZ level.

atoms and six Be–H connectivities, the  $\text{WBI}_{\text{Be-H}}$  values add up to 2.88 ( $6 \times 0.48$ ). This corroborates the formulation of three Be–H–Be 3c–2e bonds discussed above. It is also important to note that the  $\text{WBI}_{\text{Be-Be}}$  values for **3** and **4** are 0.55 and 0.59, respectively, which indicate significant direct orbital overlap between the two beryllium atoms.

### $[\text{Ng} \rightarrow \text{Be}_2\text{H}_3 \leftarrow \text{Ng}]^+$ (Ng = noble gas) with the shortest main group metal–metal distance

The ultrashort Be–Be distances in **3** and **4** mainly result from the formation of three Be–H–Be 3c–2e bonds. However, the exact Be–Be distances of 1.735 and 1.734 Å in **3** and **4** are still longer than the currently shortest Be–Be distance of 1.728 Å found in  $\text{Be}_2(\text{NLi})_2$ .<sup>9</sup> To design diberyllium complexes analogous to **3** and **4** with even shorter Be–Be distances, we considered replacing the terminal  $\text{NH}_3$  and  $\text{PH}_3$  with ligands having a minimal steric effect. Thus, we chose charge-neutral and monatomic noble gas ligands in view of previously reported theoretical and experimental studies showing viable Be–Ng bonding interactions, such as in  $[\text{Ng} \rightarrow \text{BeO}]$ ,<sup>22</sup>  $[\text{Ng} \rightarrow \text{BeS}]$ ,<sup>23</sup> and  $[\text{Ng} \rightarrow \text{Be}_2\text{O}_2 \leftarrow \text{Ng}]$ .<sup>10,24</sup> This has led to the computation of  $D_{3h}$   $[\text{Ng} \rightarrow \text{Be}_2\text{H}_3 \leftarrow \text{Ng}]^+$  (Ng = He, Ne, Ar, Kr, Xe; **5–9**) as energy minima at both B3LYP/BS1 and MP2/BS1 levels (Fig. 1). Geometry refinements at the higher CCSD(T)/BS1 level find the Be–Be distances in **5–9** to be 1.689, 1.692, 1.703, 1.707, and 1.713 Å, respectively, all of them being shorter than the Be–Be distance of 1.728 Å in  $\text{Be}_2(\text{NLi})_2$ . Most remarkably of all, complexes **5** and **6** represent the first examples having a main group metal–metal distance under 1.700 Å, which place them in the group of discrete molecular systems that have the shortest metal–metal distances. These results prompted us to further study the unsupported  $\text{Be}_2\text{H}_3^+$  core (**10**, Fig. 1), which was located as an energy minimum at both B3LYP/BS1 and MP2/BS1 levels, with a refined Be–Be distance of 1.683 Å at the CCSD(T)/BS1 level.

We have performed NBO and AdNDP analyses on **5–10** (Fig. 1 and Table 1 in the main text and Fig. S1 in the ESI†). As expected, the bonding situation in **5–9** is similar to that in **3** and **4**. There are three Be–H–Be 3c–2e bonds or a nonclassical triple bond connecting the two Be atoms. This bonding mode, along with the reduced steric effect of the noble gas ligands, causes the unprecedented ultrashort Be–Be distances in **5–9**. The total  $\text{WBI}_{\text{Ng}}$  values generally increase from 0.31 to 0.76 as Ng varies from He to Xe, which is consistent with the increasing ability of Ng to participate in bonding. The natural charges of the Ng atoms in **5–9** range from +0.14 to +0.46|e|, which suggests the dative nature of Ng–Be bonding. The bonding situation in **10** is similar to that of the  $\text{Be}_2\text{H}_3^+$  core of **5–9**.

### Stability considerations

Structures **3–10** are computationally designed novel species, and evaluation of their stabilities would give clues as to whether they could be experimentally realized.<sup>25</sup> The HOMO–LUMO gaps of **3–10** range from 6.23 to 8.51 eV, much greater than those of **1** and **2** (2.74 and 3.61 eV). Thus, **3–10** would be chemically more stable than **1** and **2**.

The thermodynamic stability of **3–10** has been studied by extensive exploration of their potential energy surfaces, and the resulting low-lying isomers, along with their relative energies, are given in the ESI (Fig. S2†). At the final CCSD(T)/BS1 level, **5** and **10** have been confirmed to be local energy minima because of the finding of their lower-energy isomers (Fig. S2 in the ESI†). Thus, it would be unlikely to experimentally realize **5** and **10**. By contrast, **3**, **4**, and **6–9** all have been proved to be global energy minima, which are 12.8, 9.7, 2.1, 4.3, 4.2, and 4.9 kcal mol<sup>−1</sup> lower than their respective second lowest isomers. Thus, they would be thermodynamically stable species.

For global minima **3**, **4**, and **6–9**, their kinetic stability is also important for experimental realization, which has been evaluated by using 100-picosecond BOMD simulations at 298 K. Structural evolution of a species during a simulation is described by the root-mean-square derivations (RMSDs) relative to its optimized geometry. As shown in Fig. 3, the RMSD plot of **6** shows an upward jump at approximately 83 ps, which correlates with a structural change to the closest isomer **6a**. A BOMD simulation for **6a** reveals interconversion between **6**

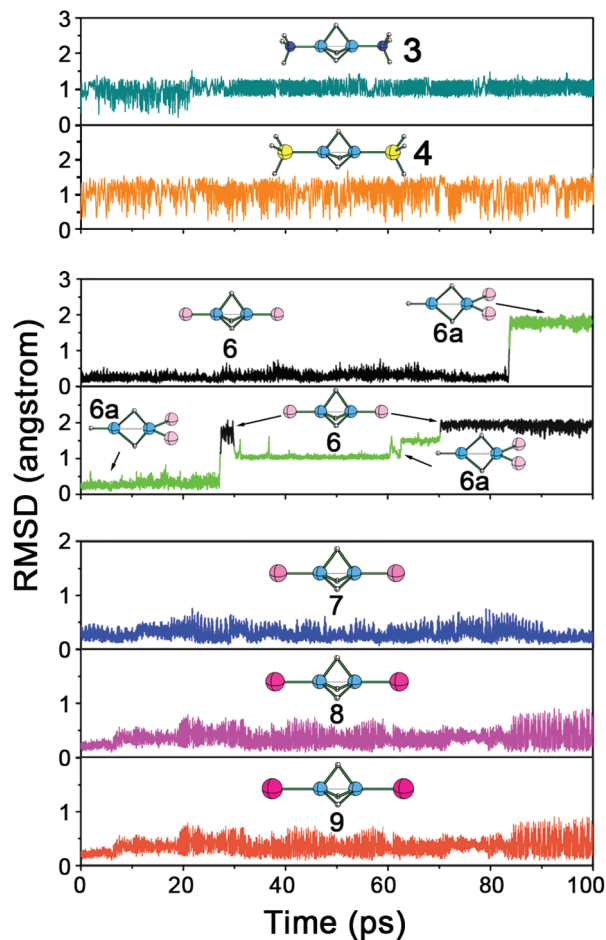


Fig. 3 Plots of RMSD (in Å) versus time (in ps) obtained with BOMD simulations for **3**, **4**, **6–9**, and **6a**.

and **6a** on the RMSD plot, suggesting that **6** and **6a** both would be observable experimentally. The RMSD plots for **3**, **4**, and **7–9** display no irreversible jumps and only minor fluctuations, indicating that they are kinetically stable.

We have further characterized **3–10** by calculating their vertical detachment energies (VDEs) and vertical electron affinities (VEAs). As shown in Table 1, the VDEs of **3–10** range from 15.15 to 18.57 eV. Such large VDE values suggest that it would be very difficult for these species to lose an electron. The VEAs of **3–5** and **7–9** are each less negative than that of  $\text{Cs}^+$  ( $-3.89$  eV), and therefore these monocations qualify as a new class of superalkali cations,<sup>26</sup> which could be used as building blocks of supersalts.<sup>27</sup> While the VEA of **6** ( $-4.30$  eV) is more negative than that of  $\text{Cs}^+$ , it is slightly less negative than that of  $\text{K}^+$  (experimentally known at  $-4.34$  eV), suggesting that **6** would be as stable as  $\text{K}^+$  towards electron gain. In comparison, the VEA of **10** ( $-6.68$  eV) indicates that this species would be less stable than **3–9** towards electron gain.

We have used **3** as an example to study the neutral free radical  $D_{3h}$   $[\text{NH}_3 \rightarrow \text{Be}_2\text{H}_3 \leftarrow \text{NH}_3]$  that arises from **3** gaining an electron. The radical has an optimized geometry closely similar to **3**, but exhibits a longer Be–Be distance (1.750 vs. 1.729 Å) at the B3LYP/BS1 level (Fig. S3 in the ESI†). In addition, the radical would be much less stable than **3**, as revealed by comparing their HOMO–LUMO gaps (0.48 vs. 7.65 eV) and VDEs (2.84 vs. 15.20 eV).

In summary, the global minimum diberyllium complexes **3**, **4**, and **6–9**, which are also kinetically stable, would have a high probability of being experimentally realized as a new class of superalkali cations that could have applications in supporting supersalts.

### Bulky analogues

Using bulky terminal ligands for the analogues of **3**, **4**, and **6–9** could have further stabilizing effect and facilitate their synthesis and isolation in condensed states (solution included). As a demonstration, we have modified the structure of **3** by replacing ammonia with the much larger triethylamine (TEA), and computed  $[\text{TEA} \rightarrow \text{Be}_2\text{H}_3 \leftarrow \text{TEA}]^+$  (**11**) as an energy minimum (Fig. 4). The Be–Be distance in **11** (1.754 Å) is slightly longer than that (1.735 Å) in **3**, as expected for increas-

ing steric repulsion introduced by the bulky ligand, but it is still well below the threshold for ultrashort metal–metal distances (1.900 Å).

The stability of **11** is manifested by its large HOMO–LUMO gap of 8.38 eV, its VDE of 13.91 eV, and its VEA of  $-1.81$  eV. Noticeably, the VEA of **11** is less negative than that of the commonly used big cation tetraethyl ammonium  $\text{N}(\text{C}_2\text{H}_5)_4^+$  (calc.  $-2.29$  eV). Such characteristics of stability, combined with the fact that the parent complex **3** is a kinetically stable global minimum, suggest that complex **11** would be a viable target for chemical synthesis.

## Conclusions

We have shown through computation that, with the aid of three bridging hydrogen atoms, a virtual triple bond can be formed between two beryllium atoms, thereby causing ultrashort Be–Be distances in  $[\text{L} \rightarrow \text{Be}_2\text{H}_3 \leftarrow \text{L}]^+$  ( $\text{L} = \text{NH}_3, \text{PH}_3, \text{He}, \text{Ne}, \text{Ar}, \text{Kr}, \text{Xe}$ ). These species are characterized for having large HOMO–LUMO gaps, high vertical detachment energies, and low vertical electron affinities. With the exception of  $[\text{He} \rightarrow \text{Be}_2\text{H}_3 \leftarrow \text{He}]^+$ , these diberyllium complexes are kinetically stable global energy minima, therefore providing potential targets for experimental realization. Noticeably, the Be–Be distance in  $[\text{Ne} \rightarrow \text{Be}_2\text{H}_3 \leftarrow \text{Ne}]^+$  is 1.692 Å, making it the first experimentally promising species with a main group metal–metal distance under 1.700 Å. Substituting bulky triethylamine (TEA) for ammonia in  $[\text{NH}_3 \rightarrow \text{Be}_2\text{H}_3 \leftarrow \text{NH}_3]^+$  leads to  $[\text{TEA} \rightarrow \text{Be}_2\text{H}_3 \leftarrow \text{TEA}]^+$ , a potentially isolable species in condensed states. In summary, this theoretical study contributes to the development of the fields of metal–metal bonding, beryllium, and noble gas chemistry. We encourage experimentalists to pursue and realize the chemically interesting and viable structures presented in this work.

## Conflicts of interest

There are no conflicts to declare.

## Acknowledgements

The authors acknowledge support for this work from the National Natural Science Foundation of China (Grant No. 21720102006, 21273140 and 21471092), the Special Program for Applied Research on Supercomputation of the NSFC-Guangdong Joint Fund (the second phase) (Grant No. U1501501), the One Hundred-Talent Program of Shanxi Province, the Program for Outstanding Innovative Teams of Higher Learning Institutions of Shanxi, the Shanxi 1331KIRT, the Foundation of the State Key Laboratory of Coal Conversion (Grant No. J17-018-610), the Shanxi University supercomputing platform, and the University of Colorado Denver. We thank Professor Mingfei Zhou for helpful discussions.

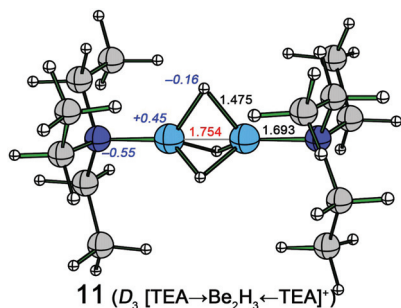


Fig. 4 B3LYP/BS1-optimized structure of **11**.

## Notes and references

- 1 (a) F. A. Cotton, *Multiple Bonds Between Metal Atoms*, Springer, New York, 2005; (b) S. T. Liddle, *Molecular Metal-Metal Bonds*, Wiley-VCH, Weinheim, 2015.
- 2 (a) F. R. Wagner, A. Noor and R. Kempe, *Nat. Chem.*, 2009, **1**, 529–536; (b) A. Noor and R. Kempe, *Inorg. Chim. Acta*, 2015, **424**, 75–82.
- 3 F. A. Cotton, N. F. Curtis, C. B. Harris, B. F. G. Johnson, S. J. Lippard, J. T. Mague, W. R. Robinson and J. S. Wood, *Science*, 1964, **145**, 1306–1308.
- 4 (a) T. Nguyen, A. D. Sutton, M. Brynda, J. C. Fettinger, G. J. Long and P. P. Power, *Science*, 2005, **310**, 844–847; (b) G. Frenking, *Science*, 2005, **310**, 796–797; (c) K. A. Kreisler, G. P. A. Yap, O. Dmitrenko, C. R. Landis and K. H. Theopold, *J. Am. Chem. Soc.*, 2007, **129**, 14162–14163; (d) C.-W. Hsu, J.-S. K. Yu, C.-H. Yen, G.-H. Lee, Y. Wang and Y.-C. Tsai, *Angew. Chem., Int. Ed.*, 2008, **47**, 9933–9936; (e) A. Noor, F. R. Wagner and R. Kempe, *Angew. Chem., Int. Ed.*, 2008, **47**, 7246–7249; (f) A. Noor, G. Glatz, R. Mueller, M. Kaupp, S. Demeshko and R. Kempe, *Z. Anorg. Allg. Chem.*, 2009, **635**, 1149–1152; (g) A. Noor and R. Kempe, *Chem. Rec.*, 2010, **10**, 413–416; (h) L.-C. Wu, C.-W. Hsu, Y.-C. Chuang, G.-H. Lee, Y.-C. Tsai and Y. Wang, *J. Phys. Chem. A*, 2011, **115**, 12602–12615; (i) Y.-L. Huang, D.-Y. Lu, H.-C. Yu, J.-S. K. Yu, C.-W. Hsu, T.-S. Kuo, G.-H. Lee, Y. Wang and Y.-C. Tsai, *Angew. Chem., Int. Ed.*, 2012, **51**, 7781–7785; (j) A. Noor, T. Bauer, T. K. Todorova, B. Weber, L. Gagliardi and R. Kempe, *Chem. – Eur. J.*, 2013, **19**, 9825–9832.
- 5 (a) V. E. Bondybey and J. H. English, *Chem. Phys. Lett.*, 1983, **94**, 443–447; (b) B. O. Roos, A. C. Borin and L. Gagliardi, *Angew. Chem., Int. Ed.*, 2007, **46**, 1469–1472; (c) G. Frenking and R. Tonner, *Nature*, 2007, **446**, 276–277.
- 6 M. Brynda, L. Gagliardi and O. R. Bjorn, *Chem. Phys. Lett.*, 2009, **471**, 1–10.
- 7 M. Kaupp and P. v. R. Schleyer, *J. Am. Chem. Soc.*, 1993, **115**, 1061–1073.
- 8 Z.-H. Cui, W.-S. Yang, L. Zhao, Y.-H. Ding and G. Frenking, *Angew. Chem., Int. Ed.*, 2016, **55**, 7841–7846.
- 9 C. Yuan, X.-F. Zhao, Y.-B. Wu and X. Wang, *Angew. Chem., Int. Ed.*, 2016, **55**, 15651–15655.
- 10 (a) Q. Zhang, W.-L. Li, L. Zhao, M. Chen, M. Zhou, J. Li and G. Frenking, *Chem. – Eur. J.*, 2017, **23**, 2035–2039; (b) W.-L. Li, J.-B. Lu, L. Zhao, R. Ponc, D. L. Cooper, J. Li and G. Frenking, *J. Phys. Chem. A*, 2018, **122**, 2816–2822.
- 11 D. Y. Zubarev and A. I. Boldyrev, *Phys. Chem. Chem. Phys.*, 2008, **10**, 5207–5217.
- 12 A. E. Reed, L. A. Curtiss and F. Weinhold, *Chem. Rev.*, 1988, **88**, 899–926.
- 13 J. V. Ortiz, V. G. Zakrzewski and O. Dolgounircheva, *Conceptual Perspectives in Quantum Chemistry*, Kluwer Academic, 1997.
- 14 (a) M. Saunders, *J. Comput. Chem.*, 2004, **25**, 621–626; (b) P. P. Bera, K. W. Sattelmeyer, M. Saunders, H. F. Schaefer and P. v. R. Schleyer, *J. Phys. Chem. A*, 2006, **110**, 4287–4290.
- 15 (a) J. M. Millam, V. Bakken, W. Chen, W. L. Hase and H. B. Schlegel, *J. Chem. Phys.*, 1999, **111**, 3800–3805; (b) X. S. Li, J. M. Millam and H. B. Schlegel, *J. Chem. Phys.*, 2000, **113**, 10062–10067.
- 16 (a) H. G. Lu and Y. B. Wu, in *GXYZ 2.0, A random search program*, Shanxi University, Taiyuan, 2015; (b) Y. B. Wu, H. G. Lu, S. D. Li and Z. X. Wang, *J. Phys. Chem. A*, 2009, **113**, 3395–3402.
- 17 The AdNDP program was downloaded freely at <http://ion.chem.usu.edu/~boldyrev/adndp.php>.
- 18 H.-J. Werner *et al.*, in *MolPro 2012.1*, University College Cardiff Consultants Limited, Cardiff, 2012.
- 19 M. J. Frisch *et al.*, in *Gaussian 09 Revision D.01*, Gaussian Inc, Wallingford, CT, 2013.
- 20 Z. Z. Qin, Q. Wang, C. X. Yuan, Y. T. Yang, X. F. Zhao, D. B. Li, P. Liu and Y. B. Wu, *Dalton Trans.*, 2018, **47**, 4707–4713.
- 21 P. Laszlo, *Angew. Chem., Int. Ed.*, 2000, **39**, 2071–2072.
- 22 (a) G. Frenking, W. Koch, J. Gauss and D. Cremer, *J. Am. Chem. Soc.*, 1988, **110**, 8007–8016; (b) C. A. Thompson and L. Andrews, *J. Am. Chem. Soc.*, 1994, **116**, 423–424.
- 23 (a) S. Borocci, N. Bronzolino and F. Grandinetti, *Chem. Phys. Lett.*, 2004, **384**, 25–29; (b) Q. Wang and X. F. Wang, *J. Phys. Chem. A*, 2013, **117**, 1508–1513.
- 24 (a) T. Kobayashi, K. Seki and T. Takayanagi, *Chem. Phys. Lett.*, 2010, **498**, 235–239; (b) T. Kobayashi, Y. Kohn, T. Takayanagi, K. Seki and K. Ueda, *Comput. Theor. Chem.*, 2012, **991**, 48–55.
- 25 R. Hoffmann, P. v. R. Schleyer and H. F. Schaefer III, *Angew. Chem., Int. Ed.*, 2008, **47**, 7164–7167.
- 26 (a) G. L. Gutsev and A. I. Boldyrev, *Chem. Phys.*, 1981, **56**, 277–283; (b) G. L. Gutsev and A. I. Boldyrev, *Chem. Phys. Lett.*, 1982, **92**, 262–266.
- 27 (a) V. Chauhan, S. Sahoo and S. N. Khanna, *J. Am. Chem. Soc.*, 2016, **138**, 1916–1921; (b) S. Giri, S. Behera and P. Jena, *J. Phys. Chem. A*, 2014, **118**, 638–645; (c) A. K. Srivastava and N. Misra, *J. Mol. Model.*, 2016, **22**, 122.